

RESEARCH ARTICLE

View Article Online
View Journal | View IssueCite this: *RSC Med. Chem.*, 2020, 11, 823

Differently fluorescence-labelled dibenzodiazepinone-type muscarinic acetylcholine receptor ligands with high M₂R affinity†

Corinna G. Gruber,  Andrea Pegoli, Christoph Müller,  Lukas Grätz, 
Xueke She and Max Keller *

A series of fluorescent dibenzodiazepinone-type muscarinic acetylcholine M₂ receptor (M₂R) ligands was synthesized using various fluorescent dyes (5-TAMRA, $\lambda_{\text{ex}}/\lambda_{\text{em}} \approx 547/576$ nm; BODIPY 630/650, $\lambda_{\text{ex}}/\lambda_{\text{em}} \approx 625/640$ nm; pyridinium dye Py-1, $\lambda_{\text{ex}}/\lambda_{\text{em}} \approx 611/665$ nm and pyridinium dye Py-5, $\lambda_{\text{ex}}/\lambda_{\text{em}} \approx 465/732$ nm). All fluorescent probes exhibited high M₂R affinity ($\text{p}K_{\text{i}}$ (radioligand competition binding): 8.75–9.62, $\text{p}K_{\text{d}}$ (flow cytometry): 8.36–9.19), a very low preference for the M₂R over the M₁ and M₄ receptors and moderate to pronounced M₂R selectivity compared to the M₃ and M₅ receptors. The presented fluorescent ligands are considered useful molecular tools for future studies using methods such as fluorescence anisotropy and BRET based MR binding assays.

Received 24th April 2020,
Accepted 20th May 2020

DOI: 10.1039/d0md00137f

rsc.li/medchem

Introduction

In the past decades, fluorescence-based techniques have been increasingly used to study membrane receptors such as G-protein coupled receptors (GPCRs), including the analysis of ligand-receptor interactions as well as the investigation of receptor expression, structure and function.^{1–4} Besides fluorescently tagged receptors, fluorescent ligands represent interesting molecular tools, which can also be used to study endogenously expressed receptors.¹ Therefore, there is a growing demand for suitable fluorescent GPCR ligands. Compared with radioligands, fluorescent ligands exhibit several advantages, such as fewer problems concerning safety risks, legal issues and waste disposal. Furthermore, they are applicable to techniques, which have become routine in many laboratories, for instance fluorescence microscopy and flow cytometry. Typically, fluorescent ligands are composed of a pharmacophore, mediating receptor affinity, a spacer/linker moiety and the fluorophore.^{1,5} The design of fluorescent ligands is not trivial, *e.g.* with respect to high receptor affinity and favorable physicochemical properties. Crucial factors are the type of the fluorescent dye (size, lipophilicity,

spectroscopic and bleaching properties, *etc.*) and the point of attachment, structure and length of the linker.^{1,6–11}

Numerous fluorescent probes have been reported for GPCRs, for instance for histamine,^{12–16} dopamine,^{17,18} opioid,^{19–22} neuropeptide Y,^{23–28} adenosine,²⁹ and neurotensin^{30,31} receptors. Concerning muscarinic acetylcholine receptors (MRs), various fluorescent MR ligands were reported, *e.g.* the BODIPY558/568-labelled derivative **1**,³² derived from the M₁ subtype preferring MR antagonist pirenzepine, the BODIPY630/650-labelled tolterodine derivative **2**,³³ the Alexa488-labelled telenzepine derived MR antagonist **3**,^{34,35} the Cy3B-labelled telenzepine analog **4**,^{34–36} and the lissamine rhodamine B-labelled AC-42 derivative **5** (ref. 37) (Fig. 1; note: in the case of **1** and **3–5** further congeners, containing the same pharmacophore but different fluorophores such as Cy3, Cy5 cascade blue or 6-carboxyfluorescein and, in part, also different linkers, were reported^{32,36–41}). The recent finding that replacement of the diethylamine moiety in the M₂R preferring dibenzodiazepinone-type MR antagonist DIBA⁴² (**6**, Fig. 1) by bulky moieties was well tolerated with respect to M₂R binding,^{43–46} gave rise to prepare a series of DIBA-derived red-emitting fluorescent MR ligands, comprising compounds **7** and **8** (Fig. 1). Whereas the indolinium-type cyanine dye containing ligands (*e.g.* **8**) were investigated in fluorescence-based techniques, the pyridinium-type cyanine dye containing probes (*e.g.* **7**) were only characterized with respect to M₁R–M₅R affinity in radioligand competition binding studies.⁴⁷ In the present study, a new series of

Institute of Pharmacy, Faculty of Chemistry and Pharmacy, University of Regensburg, Universitätsstrasse 31, D-93053 Regensburg, Germany.

E-mail: max.keller@ur.de

† Electronic supplementary information (ESI) available: Fig. S1–S4; RP-HPLC chromatograms of compounds 15–20; ¹H-NMR spectra of compounds 15–20. See DOI: 10.1039/d0md00137f

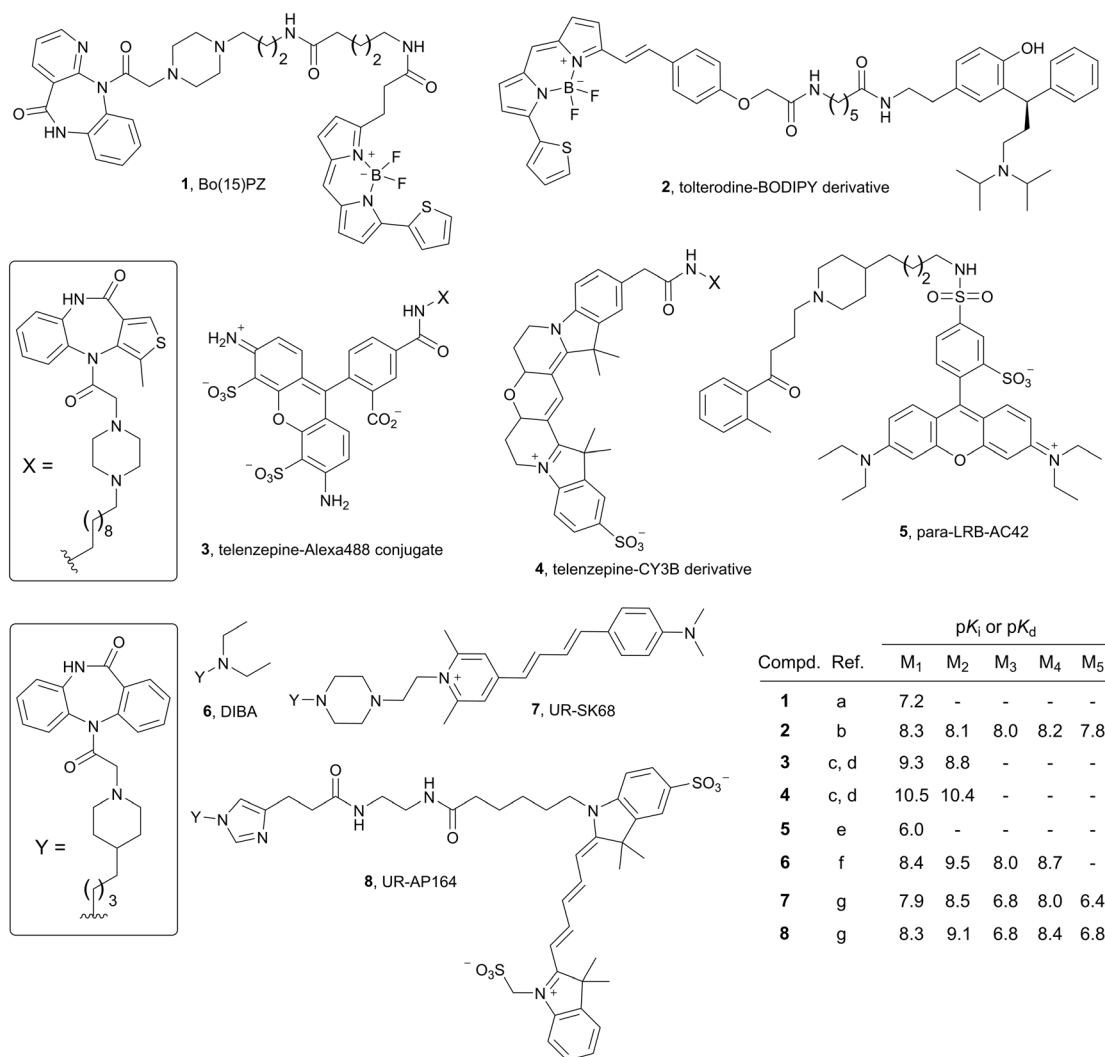


Fig. 1 Structures and MR binding data of the reported fluorescent probes 1–5, being non-selective MR ligands (1–4) or showing a slight preference for the M₁R (2),³³ and structures and MR affinities of the M₂R preferring dibenzodiazepinone-type MR ligands DIBA and the DIBA-derived fluorescent probes 7 and 8.⁴⁷ (Note: binding data for all MR subtypes were not reported in all cases). ^a Tahtaoui *et al.* (the reported K_i value was converted to a pK_i value),³² ^b Jones *et al.* (reported K_i values were converted to pK_i values),³³ ^c Hern *et al.* (reported K_i values were converted to pK_i values),³⁴ ^d Nenasheva *et al.*,³⁵ ^e Daval *et al.*,³⁷ ^f Gitler *et al.* (reported K_i values were converted to pK_i values),⁴² ^g She *et al.*⁴⁷

fluorescently labelled dibenzodiazepinone-type MR ligands was prepared using various fluorescent dyes (TAMRA, BODIPY630/650, pyridinium-type cyanine dyes Py-1 and Py-5). The probes were characterized with respect to M₁R–M₅R affinity (radioligand competition binding) and by flow cytometric saturation binding studies, the latter including the reported ligand 7.

Results and discussion

Chemistry

A set of six fluorescent dibenzodiazepinone-type MR ligands (15–20) was prepared from the previously reported amine-functionalized dibenzodiazepinone derivatives **9** (ref. 43) and **10** (ref. 46) using four different fluorescent dyes: 5-TAMRA succinimidyl ester (**11**), BODIPY 630/650 succinimidyl ester (**12**), and the pyrylium dyes Py-1 (**13**)⁴⁸ and Py-5 (**14**)⁴⁸ (*cf.* Fig. 2).

Treatment of **9** with the fluorescent dyes **11–14** in the presence of DIPEA or triethylamine yielded the fluorescent ligands **15–18** (Scheme 1). Likewise, treatment of **10** with **13** or **11** gave the fluorescent probes **19** and **20**, respectively (Scheme 1). Purification by preparative RP-HPLC afforded **15–20** with high purities (≥96%, HPLC analysis at 220 nm). All fluorescent ligands were investigated with respect to their chemical stability in PBS pH 7.4. Whereas compounds **15**, **16**, **19** and **20** showed no decomposition within the incubation period of 48 h (Fig. S2, ESI[†]), compounds **17** and **18** showed minor decomposition after 24 h (after 24 h, peak areas (220 nm) of **17** and **18** amounted to 94% and 90%, respectively, of the total peak area).

Radioligand competition binding studies with [³H]NMS

M₁R–M₅R affinities of **15–20** were determined at intact CHO–hM_xR cells (x = 1–5) using the orthosteric non-selective MR

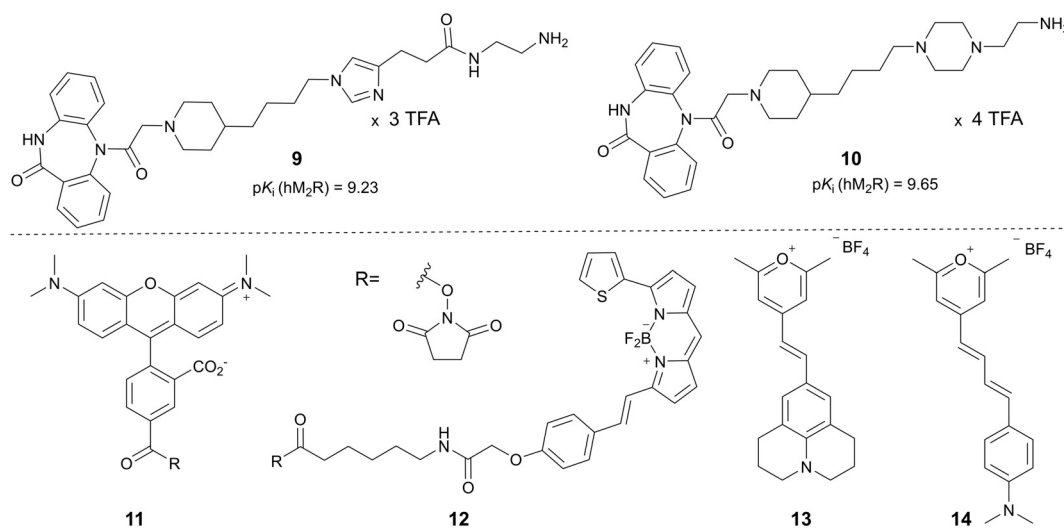
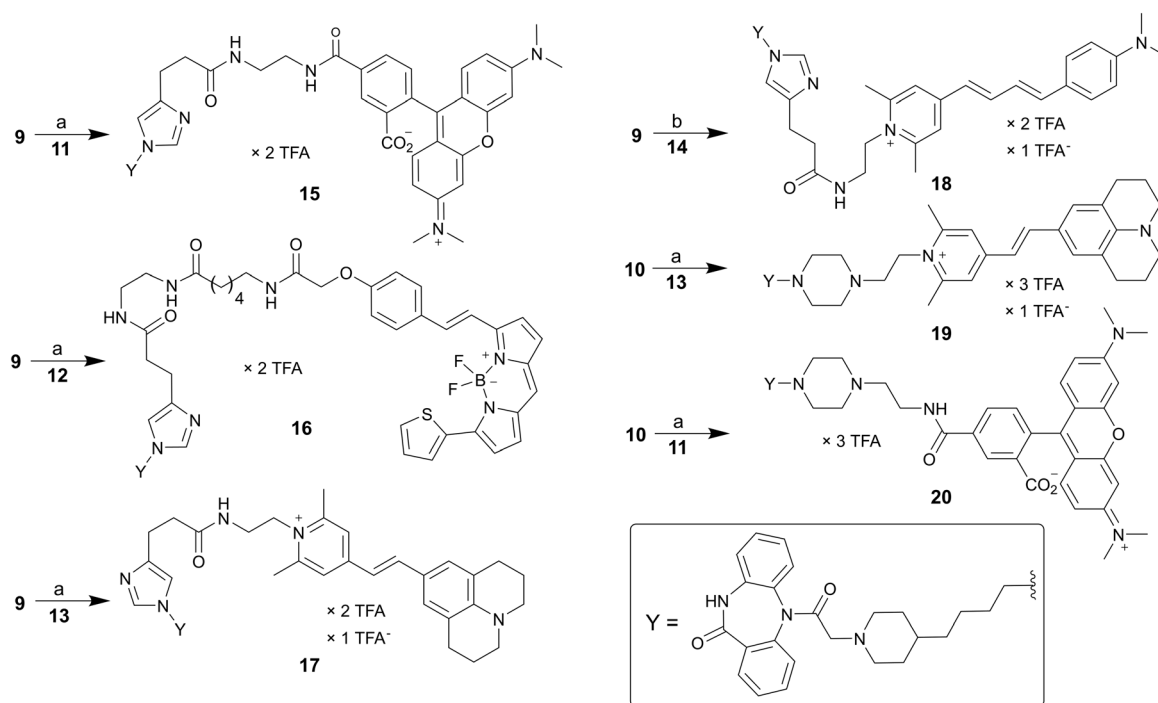


Fig. 2 Structures and M₂R affinities of the previously described DIBA derived amine-functionalized precursors **9** and **10**,^{43,46} and structures of the fluorescent dyes **11–14**, which were used for the preparation of the fluorescent MR ligands **15–20** (note: M₂R binding data of **9**, reported as pIC₅₀ value,⁴³ were re-analyzed to obtain the pK_i value).



Scheme 1 Synthesis of the fluorescent dibenzodiazepinone-type MR ligands **15–20**, labelled with TAMRA (**15**, **20**), BODIPY630/650 (**16**), pyrylium/pyridinium dye Py-1 (**17**, **19**) or Py-5 (**18**). Reagents and conditions: (a): DIPEA, DMF, rt, 2 h, 31% (**15**), 23% (**16**), 16% (**17**), 23% (**19**), 66% (**20**); (b) triethylamine, DMF, rt, 2 h, 28% (**18**).

antagonist [³H]NMS as radioligand. Compounds **15–20** were capable of completely displacing [³H]NMS from all MR subtypes (Fig. 3 and Fig. S1, ESI[†]). The corresponding pK_i values are listed in Table 1. All fluorescent ligands **15–20** exhibited high M₂R affinity (pK_i values >8.7). The TAMRA-labelled compound **20** showed the highest M₂R affinity (pK_i: 9.62). For this fluorescent ligand, sigmoidal [³H]NMS displacement curves (M₁R–M₅R) are shown in

Fig. 3B. As in the case of the recently reported series of dibenzodiazepinone-type fluorescent ligands including **7** and **8**,⁴⁷ **15–20** showed no or very low preference for the M₂R compared to the M₁ and M₄ receptor, but moderate to pronounced M₂R selectivity towards the M₃ and M₅ subtypes (Table 1). Compound **20** exhibited the highest, but still moderate preference for the M₂R over the M₁R and M₄R.

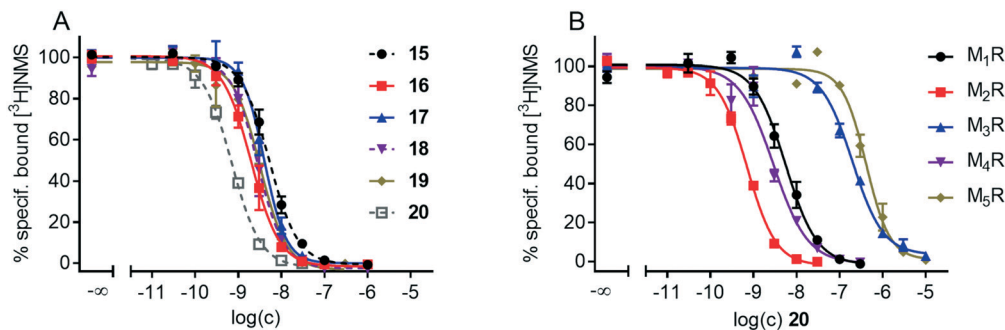


Fig. 3 (A) Concentration-dependent effects of **15**–**20** on [^3H]NMS ($c = 0.2 \text{ nM}$) equilibrium M_2R binding determined at intact CHO-h M_2R cells. (B) Radioligand displacement curves obtained from competition binding experiments with [^3H]NMS (0.2 nM (M_1R , M_2R , M_3R), 0.1 nM (M_4R) or 0.3 nM (M_5R)) and compound **20** performed at intact CHO-h M_xR cells ($x = 1$ – 5). M_2R data are the same as in A. Data in A and B represent mean values \pm SEM from two (**20**, M_5R) or at least three independent experiments (each performed in triplicate).

Table 1 M_1 – M_5 receptor binding data (pK_i values) of compounds **7** and **15**–**20** obtained from radioligand competition binding studies, and M_2R binding data (pK_d values) from flow cytometric saturation binding experiments

Compd.	pK_i^a					pK_d^b
	M_1R	M_2R	M_3R	M_4R	M_5R	M_2R
7 (ref. 47)	7.86	8.52	6.83	8.02	6.41	8.63 ± 0.08
15 (UR-CG072)	8.21 ± 0.02	8.75 ± 0.07	6.89 ± 0.06	8.43 ± 0.07	6.56 ± 0.10	8.36 ± 0.09
16 (UR-CG073)	9.00 ± 0.13	9.16 ± 0.10	7.43 ± 0.13	9.38 ± 0.05	8.00 ± 0.08	8.41 ± 0.10
17 (UR-CG074)	8.15 ± 0.05	8.87 ± 0.08	7.16 ± 0.01	8.58 ± 0.08	7.39 ± 0.07	8.70 ± 0.04
18 (UR-AP175)	8.31 ± 0.04	9.04 ± 0.15	7.07 ± 0.04	8.37 ± 0.04	7.15 ± 0.06	8.74 ± 0.13
19 (UR-CG135)	8.32 ± 0.03	9.02 ± 0.10	7.20 ± 0.15	8.57 ± 0.01	6.90 ± 0.03	9.19 ± 0.03
20 (UR-MK342)	8.59 ± 0.10	9.62 ± 0.04	7.09 ± 0.06	9.01 ± 0.03	6.75 ± 0.05	8.86 ± 0.06

^a Determined by competition binding with [^3H]NMS (K_d values/applied concentrations: M_1 , $0.17/0.2 \text{ nM}$; M_2 , $0.10/0.2 \text{ nM}$; M_3 , $0.12/0.2 \text{ nM}$; M_4 , $0.052/0.1 \text{ nM}$; M_5 , $0.20/0.3 \text{ nM}$) at whole CHO-h M_xR cells ($x = 1$ – 5) at $23 \text{ }^\circ\text{C}$. Means \pm SEM from two (**20**, M_5R) or at least three independent experiments (each performed in triplicate). ^b Determined by flow cytometric saturation binding experiments at intact CHO-h M_2R cells at $22 \text{ }^\circ\text{C}$. Means \pm SEM from two (**20**) or at least three independent experiments (performed in duplicate).

Fluorescence properties

Excitation and corrected emission spectra of **15**–**20**, recorded in PBS containing 1% bovine serum albumin (BSA), are shown in ESI† Fig. S3 and the respective excitation and emission maxima are summarized in Table 2. It should be noted that compounds **7** and **18**, both labelled with the pyrylium/pyridinium-type fluorescent dye Py-5 are perfectly suited for an excitation with an argon laser (488 nm), belonging to the standard equipment of many instruments. Compound **16** is well suited for an excitation with the commonly used red diode laser (*ca.* 635 nm), and **15**, **17**, **19** and **20** require green light for an optimal excitation (*cf.* Table 2).

Table 2 Excitation and emission maxima of the fluorescent ligands **7**, **15**–**20** determined in PBS containing 1% BSA

Compd.	Dye	$\lambda_{\text{ex}}/\lambda_{\text{em}}$
7 (ref. 47)	Pyridinium cyanine (Py-5)	484/643
15	5-TAMRA	557/583
16	BODIPY 630/650	639/647
17	Pyridinium cyanine (Py-1)	526/602
18	Pyridinium cyanine (Py-5)	483/634
19	Pyridinium cyanine (Py-1)	526/604
20	5-TAMRA	550/583

Flow cytometric M_2R saturation binding studies

M_2R affinities of the fluorescent ligands **7** and **15**–**20** were also determined by flow cytometric saturation binding studies at intact CHO-h M_2R cells at $22 \text{ }^\circ\text{C}$ using a FACSCantoII (**7**, **15**–**19**) or a FACSCalibur (**20**) flow cytometer, both equipped with two light sources (argon and red diode laser) (*cf.* Fig. 4). For these experiments, an incubation period of 2 h was applied because association binding experiments with recently reported radio- and fluorescence labelled dibenzodiazepinone-type MR ligands at intact CHO-h M_2R cells or cell homogenates revealed that equilibrium was reached within 2 h.^{45–47} The obtained pK_d values of compounds **7** and **15**–**20** were in good agreement with the corresponding pK_i values obtained from competition binding studies with [^3H]NMS (Table 1).

Conclusion

The synthesized series of fluorescence-labelled dibenzodiazepinone-type M_2R ligands represents an extension of a recently reported set of fluorescent MR ligands⁴⁷ with respect to the type of attached fluorescent dyes. As the 5-TAMRA fluorophore exhibits a fluorescence

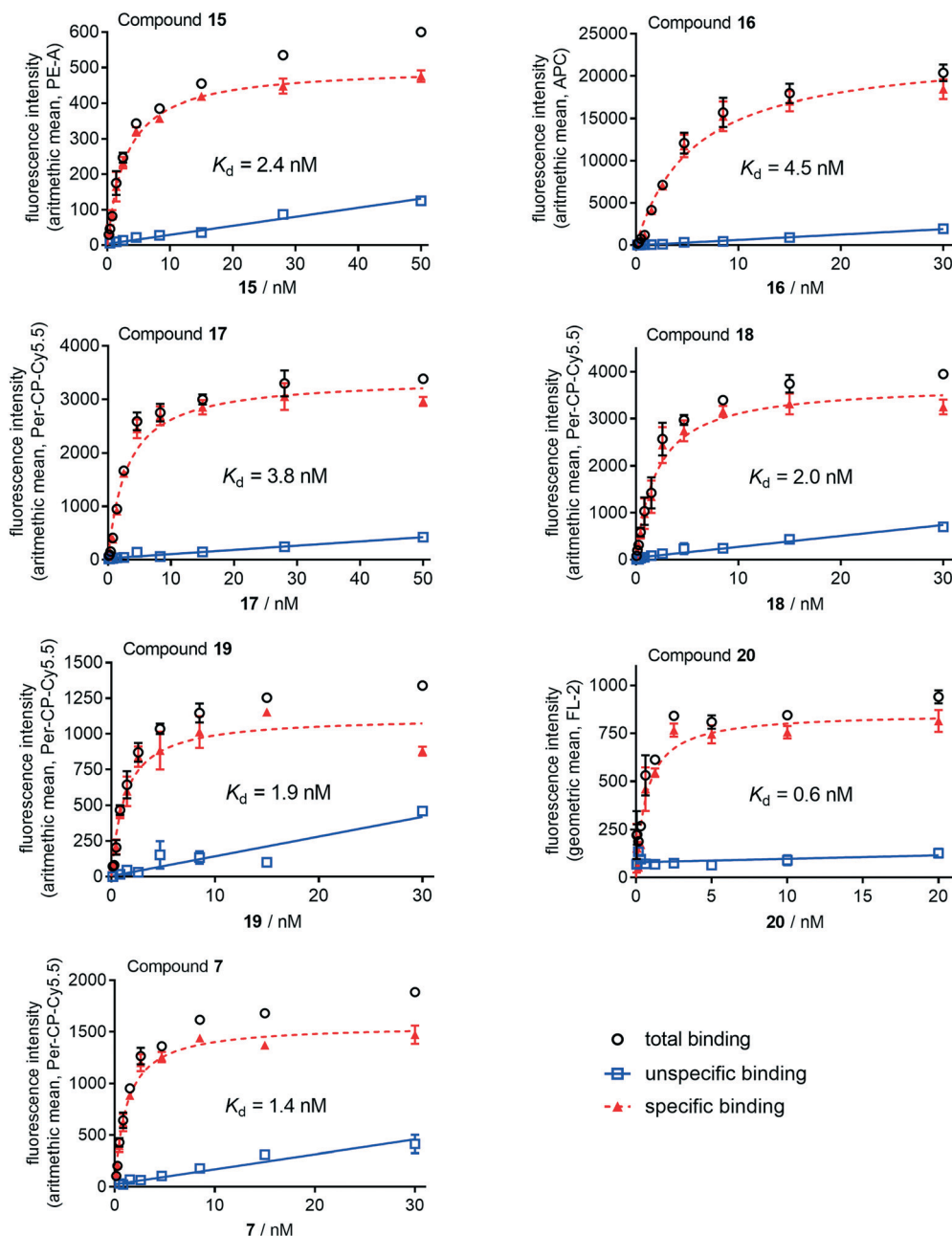


Fig. 4 Representative saturation isotherms (specific binding, dashed line) obtained from flow cytometric saturation binding experiments performed with **7** and **15–20** at intact CHO-hM₂R cells. Unspecific binding was determined in the presence of atropine (**21**, for structure see Fig. S4, ESI†) used in 500- or 1000-fold excess. Cells were incubated with the fluorescent ligands at 22 °C in the dark for 2 h. Experiments were performed in duplicate. Measurements were performed on a FACSCantoll (**7**, **15–19**) or a FACSCalibur (**20**) flow cytometer (Becton Dickinson). Used laser lines/emission filters: **15**, 488 nm/585 ± 21 nm (PE channel); **16**, 488 nm/660 ± 10 nm (APC channel); **7** and **17–19**, 488 nm/670 ± 65 nm (PerCP-Cy5 channel); **20**, 488 nm/585 ± 21 nm (channel FL-2). Data represent mean values ± SEM (total and unspecific binding) or calculated values ± propagated error (specific binding). Note: total and unspecific binding data represent autofluorescence-corrected data.

life-time (*ca.* 2.4 ns), which is well compatible with fluorescence anisotropy measurements,⁴⁹ the TAMRA-labelled MR ligands (**15**, **20**) will be characterized in fluorescence anisotropy-based assays in future studies including real-time kinetic measurements. Furthermore, the Py-5 labelled probes (**7**, **18**), exhibiting an excitation maximum around 480 nm and a large Stokes shift (emission maximum ≈ 630 nm) should be ideal probes for a recently reported BRET-based

GPCR binding assay,⁴ requiring fusion of the NanoLuciferase (λ_{max} (bioluminescence) ≈ 460 nm) to the M₂R.

Experimental section

General experimental conditions

All chemicals and solvents were purchased from commercial suppliers and were used without further purifications.

Acetonitrile for HPLC (gradient grade) was obtained from Merck (Darmstadt, Germany) or Sigma-Aldrich (Taufkirchen, Germany). Atropine (**21**) was purchased from Sigma-Aldrich. The 5-carboxytetramethylrhodamine succinimidyl ester (**11**) was purchased from ABCR (Karlsruhe, Germany) and BODIPY 630/650 succinimidyl ester (**12**) was purchased from Lumiprobe (Hannover, Germany). The pyrylium dyes **9** and **10** were prepared according to described procedures.⁴⁸ [³H] NMS (specific activity = 80 Ci/mmol) was purchased from American Radiolabeled Chemicals Inc. (St. Louis, MO) via Hartman Analytics (Braunschweig, Germany). Millipore water was used throughout for the preparation of stock solutions and HPLC eluents. Polypropylene reaction vessels (1.5 or 2 mL) with screw cap (Süd-Laborbedarf, Gauting, Germany) were used for the synthesis of all fluorescent ligands and for the preparation and storage of stock solutions. NMR spectra were recorded on a Bruker Avance III HD 600 equipped with a cryogenic probe (14.1 T; ¹H: 600 MHz) (Bruker, Karlsruhe, Germany). Abbreviations for the multiplicities of the signals are s (singlet), d (doublet), t (triplet), m (multiplet) and brs (broad singlet). High-resolution mass spectrometry (HRMS) analysis was performed on an Agilent 6540 UHD Accurate-Mass Q-TOF LC/MS system (Agilent Technologies, Santa Clara, CA) using an ESI source. Preparative HPLC of compounds **15–20** was performed with a Prep 150 LC system from Waters (Eschborn, Germany) consisting of a binary gradient module, a 2489 UV/visible detector, and a Waters fraction collector III. Compounds **18** and **20** were purified with a preparative HPLC system from Knauer (Berlin, Germany) consisting of two K-1800 pumps and a K-2001 detector. For both systems a Kinetex-XB C18 (5 μm, 250 mm × 21 mm; Phenomenex, Aschaffenburg, Germany) served as stationary phases at a flow rate of 20 mL min⁻¹. Mixtures of 0.1% aq TFA and acetonitrile were used as mobile phase. The detection wavelength was set to 220 nm throughout. The solvent of collected fractions was removed by lyophilization using a Scanvac freeze drying apparatus (Labogene, Allerød, Denmark) equipped with a RZ 6 rotary vane vacuum pump (Vacuubrand, Wertheim, Germany). Analytical HPLC analysis was performed with a system from Agilent Technologies composed of a 1290 Infinity binary pump equipped with a degasser, a 1290 Infinity autosampler, a 1290 Infinity thermostated column compartment, a 1260 Infinity diode array detector, and a 1260 Infinity fluorescence detector. A Kinetex-XB C18 (2.6 μm, 100 × 3 mm; Phenomenex) was used as stationary phase at a flow rate of 0.6 mL min⁻¹. Mixtures of 0.04% aq TFA (A) and acetonitrile (B) were used as mobile phase. The following linear gradients were applied: compounds **15–17**, **19** and **20** (purity): 0–12 min: A/B 90:10 to 55:45, 12–16 min: 55:45 to 5:95, 16–20 min: 5:95; compound **18** (purity): 0–15 min: A/B 90:10 to 50:50, 15–19 min: 50:50 to 5:95; 20–22 min: 5:95; compounds **15–20** (chemical stabilities): 0–20 min: A/B 90:10 to 35:65, 20–22 min: 35:65 to 5:95, 22–26 min: 5:95. For all analytical HPLC runs the oven temperature was set to 25 °C, the injection volume was 20 μL and detection was performed at 220 nm.

The stock solutions (final concentration: 1 mM) of fluorescent ligands were prepared in DMSO and were stored at -78 °C.

Annotation concerning the ¹H-NMR spectra of the dibenzodiazepinone derivatives **15–20**: due to a slow rotation about the exocyclic amide group of the diazepinone ring on the NMR time scale, two isomers (ratios provided in the experimental protocols) were evident in the ¹H-NMR spectra.

Compounds characterization

All target compounds (**15–20**) were characterized by ¹H-NMR spectroscopy, HRMS, and RP-HPLC analysis. The HPLC purity of all fluorescent ligands amounted to ≥96% (220 nm) (chromatograms shown in the electronic ESI†).

Experimental synthetic protocols and analytical data of compounds 15–20

2-(6-(Dimethylamino)-3-(dimethyliminio)-3H-xanthen-9-yl)-5-((2-(3-(1-(4-(1-(2-oxo-2-(11-oxo-10,11-dihydro-5H-dibenzo[*b,e*][1,4]diazepin-5-yl)ethyl)piperidin-4-yl)butyl)-1H-imidazol-4-yl)propanamido)ethyl)carbamoyl)benzoate bis-(hydrotrifluoroacetate) (15**).** The reaction was carried out in a 1.5 mL propylene reaction vessel equipped with a micro stir bar. Amine precursor **9** (tris(hydrotrifluoroacetate), 14.5 mg, 0.016 mmol) and DIPEA (10.3 mg, 14 μL, 0.089 mmol) were dissolved in anhydrous DMF (90 μL) followed by the addition of **11** (4.2 mg, 0.008 mmol) dissolved in anhydrous DMF (50 μL). After stirring at room temperature in the dark for 2 h, 10% aq TFA (corresponding to 0.09 mmol of TFA) were added.

Purification of the product by preparative HPLC (gradient: 0–40 min: 0.1% aq TFA/acetonitrile 81:19-28:72, *t_R* = 13 min) yielded compound **15** as a red solid (3.0 mg, 31%). Ratio of configurational isomers evident in the ¹H-NMR spectrum: *ca.* 1.5:1. ¹H-NMR (600 MHz, MeOH-*d*₄): δ (ppm) 1.33–1.40 (m, 4H), 1.44–1.57 (m, 3H), 1.85–1.93 (m, 3H), 1.93–1.99 (m, 1H), 2.62 (t, 2H, *J* 7.2 Hz), 2.89–2.98 (m, 1H), 3.00 (t, 2H, *J* 7.2 Hz), 3.02–3.10 (m, 1H), 3.45 (t, 3H, *J* 6.0 Hz, interfering with the ¹³C satellite of the solvent residual peak), 3.56 (t, 2H, *J* 6.1 Hz), 3.72 (d, 1.4H, *J* 7.2 Hz), 3.80 (d, 0.60H, *J* 17 Hz), 4.18 (t, 2H, *J* 7.2 Hz), 4.37–4.46 (m, 1H), 7.0–7.02 (m, 2H), 7.03–7.08 (m, 2H), 7.11–7.14 (m, 2H), 7.24–7.36 (m, 2H), 7.36–7.43 (m, 1.4H), 7.46–7.55 (m, 3.2H), 7.59–7.65 (m, 1.4H), 7.65–7.70 (m, 0.6H), 7.72–7.77 (m, 0.4H), 7.87–7.92 (m, 0.6H), 7.95–7.99 (m, 0.4H), 8.22–8.26 (m, 1H), 8.73–8.77 (m, 1H), 8.80 (s, 1H). Note: exchangeable protons (NH, OH) were not apparent. The proton signals of the four methyl groups (12 protons) were not apparent due to an interference with the solvent residual peak. HRMS (ESI): *m/z* [*M* + *H*]⁺ calcd. for [C₅₇H₆₂N₉O₇]⁺: 984.4767, found: 984.4757. RP-HPLC (220 nm): 97% (*t_R* = 7.40 min, *k* = 8.7). C₅₇H₆₁N₉O₇·C₄H₂F₆O₄ (984.17 + 228.04).

(E)-6-(2-(4-(2-(5,5-Difluoro-7-(thiophen-2-yl)-5H-4λ⁴,5λ⁴-dipyrrolo[1,2-*c*:2',1'-*f*][1,3,2]diazaborinin-3-yl)vinyl)phenoxy)-acetamido)-N-(2-(3-(1-(4-(1-(2-oxo-2-(11-oxo-10,11-dihydro-5H-dibenzo[*b,e*][1,4]diazepin-5-yl)ethyl)piperidin-4-yl)butyl)-1H-

imidazol-4-yl)propanamido)ethyl)hexanamide bis-(hydrotrifluoroacetate) (16). Compound **16** was prepared from **9** (tris(hydrotrifluoroacetate), 8.6 mg, 0.009 mmol) and **12** (3.1 mg, 0.0047 mmol) according to the procedure used for the synthesis of **15**. DIPEA: 6.1 mg, 8.2 μ L, 0.047 mmol. Purification of the product by preparative HPLC (gradient: 0–40 min: 0.1% aq TFA/acetonitrile 81:19–19:81, t_R = 22 min) yielded **16** as a blue solid (1.35 mg, 23%). Ratio of configurational isomers evident in the $^1\text{H-NMR}$ spectrum: *ca.* 1.5:1. $^1\text{H-NMR}$ (600 MHz, MeOH-d_4): δ (ppm) 1.25–1.33 (m, 7H), 1.42–1.51 (m, 2H), 1.52–1.64 (m, 4H), 1.77–1.93 (m, 4H), 2.16 (t, 2H, J 7.2 Hz), 2.52 (t, 2H, J 7.2 Hz), 2.81–2.88 (m, 1H), 2.92 (t, 2H, J 7.2 Hz), 2.95–3.02 (m, 1H), 3.21–3.25 (m, 4H, interfering with the solvent peak), 3.26–3.28 (m, 3H, interfering with the solvent peak), 3.36–3.41 (m, 1H, interfering with the ^{13}C satellite of the solvent residual peak), 3.66–3.72 (m, 1H); 4.09 (t, 2H, J 7.2 Hz), 4.33–4.42 (m, 1H), 4.58 (s, 2H), 6.87 (d, 1H, J 4.2 Hz), 7.03–7.07 (m, 2H), 7.15 (d, 2H, J 4.2 Hz), 7.19–7.23 (m, 2H), 7.25–7.35 (m, 3H), 7.39 (s, 1H), 7.39–7.42 (m, 0.4H), 7.46–7.51 (m, 1.6H), 7.52–7.66 (m, 7H), 7.66–7.71 (m, 0.6H), 7.71–7.76 (m, 0.4H), 7.89–7.94 (m, 0.6H), 7.95–8.00 (m, 0.4H), 8.11 (d, 1H, J 3.9 Hz), 8.72 (s, 1H). Note: exchangeable protons (NH) were not apparent. HRMS (ESI): m/z $[\text{M} + \text{H}]^+$ calcd. for $[\text{C}_{61}\text{H}_{68}\text{BF}_2\text{N}_{10}\text{O}_6\text{S}]^+$: 1117.5100, found: 1117.5110. RP-HPLC (220 nm): 99% (t_R = 7.62 min, k = 9.0). $\text{C}_{61}\text{H}_{67}\text{BF}_2\text{N}_{10}\text{O}_6\text{S}\cdot\text{C}_4\text{H}_2\text{F}_6\text{O}_4$ (1117.14 + 228.04).

(E)-2,6-Dimethyl-1-(2-(3-(1-(4-(1-(2-oxo-2-(11-oxo-10,11-dihydro-5H-dibenzo[*b,e*][1,4]diazepin-5-yl)ethyl)piperidin-4-yl)butyl)-1H-imidazol-4-yl)propanamido)ethyl)-4-(2-(2,3,6,7-tetrahydro-1H,5H-pyrido[3,2,1-*ij*]quinolin-9-yl)vinyl)pyridin-1-ium bis(hydrotrifluoroacetate) trifluoroacetate (17). Compound **17** was prepared from **9** (tris(hydrotrifluoroacetate), 28 mg, 0.031 mmol) and **13** (17 mg, 0.043 mmol) according to the procedure used for the synthesis of **15**. DIPEA: 40 mg, 53 μ L, 0.31 mmol. Purification of the product by preparative HPLC (gradient: 0–40 min: 0.1% aq TFA/acetonitrile 85:15–38:62, t_R = 23 min) yielded **17** as a red solid (5.4 mg, 16%). Ratio of configurational isomers evident in the $^1\text{H-NMR}$ spectrum: *ca.* 1.5:1. $^1\text{H-NMR}$ (600 MHz, MeOH-d_4): δ (ppm) 1.32–1.39 (m, 4H), 1.41–1.56 (m, 3H), 1.81–1.92 (m, 3H), 1.93–2.00 (m, 5H), 2.60 (t, 2H, J 7.3 Hz), 2.75 (t, 4H, J 6.6 Hz), 2.82 (s, 6H), 2.89–2.96 (m, 3H), 2.99–3.06 (m, 1H), 3.45 (t, 1H, J 13 Hz, interfering with the ^{13}C satellite of the solvent residual peak), 3.62 (t, 2H, J 7.2 Hz), 3.69–3.81 (m, 2H), 4.14 (t, 2H, J 7.3 Hz), 4.38 (s, 0.4 H), 4.40–4.42 (m, 0.6H), 4.43–4.48 (m, 2H), 6.83 (d, 1H, J 16 Hz), 7.13 (s, 2H), 7.25–7.41 (m, 3.6H), 7.47–7.55 (m, 2.4H), 7.61–7.67 (m, 4H), 7.67–7.71 (m, 0.6H), 7.73–7.77 (m, 0.4H), 7.89–7.92 (m, 0.6H), 7.97 (d, 0.4H, J 7.6 Hz), 8.79 (s, 1H). Note: exchangeable protons (NH) were not apparent. The proton signals of two methylene groups (4 protons) of the fluorophore were not apparent due to an interference with the solvent residual peak. HRMS (ESI): m/z $[\text{M}]^+$ calcd. for $[\text{C}_{53}\text{H}_{63}\text{N}_8\text{O}_3]^+$: 859.5018, found: 859.5026. RP-HPLC (220 nm): 96% (t_R = 9.5 min, k = 12.0). $\text{C}_{53}\text{H}_{63}\text{N}_8\text{O}_3\cdot\text{C}_2\text{F}_3\text{O}_2\cdot\text{C}_4\text{H}_2\text{F}_6\text{O}_4$ (860.14 + 341.07).

4-((1E,3E)-4-(4-(Dimethylamino)phenyl)buta-1,3-dien-1-yl)-2,6-dimethyl-1-(2-(3-(1-(4-(1-(2-oxo-2-(11-oxo-10,11-dihydro-5H-dibenzo[*b,e*][1,4]diazepin-5-yl)ethyl)piperidin-4-yl)butyl)-1H-imidazol-4-yl)propanamido)ethyl)pyridin-1-ium bis-(hydrotrifluoroacetate)trifluoroacetate (18). Compound **18** was prepared from **9** (tris(hydrotrifluoroacetate), 6.4 mg, 0.007 mmol) and **14** (7.7 mg, 0.021 mmol) following the procedure used for the synthesis of **15**, but triethylamine (7.1 mg, 9.8 μ L, 0.07 mmol) was used instead of DIPEA. Purification of the product by preparative HPLC (gradient: 0–40 min: 0.1% aq TFA/acetonitrile 81:19–40:60, t_R = 16 min) yielded **18** as a red solid (2.3 mg, 28%). Ratio of configurational isomers evident in the $^1\text{H-NMR}$ spectrum: *ca.* 1.5:1. $^1\text{H-NMR}$ (600 MHz, MeOH-d_4): δ (ppm) 1.32–1.38 (m, 4H), 1.39–1.55 (m, 3H), 1.82–1.89 (m, 3H), 1.89–1.97 (m, 1H), 2.60 (t, 2H, J 7.3 Hz), 2.85 (s, 6H), 2.89–2.95 (m, 3H), 3.02 (s, 7H), 3.44 (t, 1H, J 13 Hz, interfering with the ^{13}C satellite of the solvent residual peak), 3.64 (t, 2H, J 7.2 Hz), 3.68–3.80 (m, 2H), 4.15 (t, 2H, J 7.4 Hz), 4.36–4.45 (m, 1H), 4.50 (t, 2H, J 7.1 Hz), 6.57 (d, 1H, J 15 Hz), 6.76 (d, 2H, J 8.8 Hz), 6.92–6.99 (m, 1H), 7.02 (d, 1H, J 15 Hz), 7.25–7.41 (m, 3.6H), 7.44 (d, 2H, J 8.9 Hz), 7.47–7.55 (m, 2.4H), 7.61–7.66 (m, 1.6H), 7.66–7.72 (m, 3H), 7.73–7.78 (m, 0.4H), 7.89–7.92 (m, 0.6H), 7.98 (d, 0.4H, J 8.4 Hz), 8.79 (s, 1H). Note: exchangeable protons (NH) were not apparent. HRMS (ESI): m/z $[\text{M}]^+$ calcd. for $[\text{C}_{51}\text{H}_{61}\text{N}_8\text{O}_3]^+$: 833.4861, found 833.4879. RP-HPLC (220 nm): 98% (t_R = 8.4 min, k = 10.0). $\text{C}_{51}\text{H}_{61}\text{N}_8\text{O}_3\cdot\text{C}_2\text{F}_3\text{O}_2\cdot\text{C}_4\text{H}_2\text{F}_6\text{O}_4$ (834.10 + 341.07).

(E)-2,6-Dimethyl-1-(2-(4-(4-(1-(2-oxo-2-(11-oxo-10,11-dihydro-5H-dibenzo[*b,e*][1,4]diazepin-5-yl)ethyl)piperidin-4-yl)butyl)piperazin-1-yl)ethyl)-4-(2-(2,3,6,7-tetrahydro-1H,5H-pyrido[3,2,1-*ij*]quinolin-9-yl)vinyl)pyridin-1-ium tris-(hydrotrifluoroacetate)trifluoroacetate (19). Compound **19** was prepared from **10** (17 mg, 0.018 mmol), and **13** (10 mg, 0.026 mmol) according to the procedure used for the synthesis of **15**. DIPEA: 23 mg, 31 μ L, 0.18 mmol. Purification of the product by preparative HPLC (gradient: 0–40 min: 0.1% aq TFA/acetonitrile 81:19–29:71, t_R = 18 min) yielded **19** as a red solid (5.1 mg, 23%). Ratio of configurational isomers evident in the $^1\text{H-NMR}$ spectrum: *ca.* 1.5:1. $^1\text{H-NMR}$ (600 MHz, MeOH-d_4): δ (ppm) 1.33–1.57 (m, 7H), 1.68–1.77 (m, 2H), 1.90–2.00 (m, 6H), 2.56–2.63 (m, 2H), 2.75 (t, 4H, J 6.3 Hz), 2.80 (s, 6H), 2.92 (t, 3H, J 6.7 Hz), 2.98–3.18 (m, 8H), 3.45 (t, 1H, J 12 Hz, interfering with the ^{13}C satellite of the solvent residual peak), 3.52–3.59 (m, 2H), 3.70–3.82 (m, 2H), 4.37–4.46 (m, 1H), 4.51 (t, 2H, J 6.6 Hz), 6.84 (d, 1H, J 16 Hz), 7.13 (s, 2H), 7.24–7.32 (m, 1H), 7.32–7.36 (m, 1H), 7.40 (t, 0.4H, J 7.7 Hz), 7.47–7.56 (m, 2.2H), 7.60–7.72 (m, 5H), 7.76 (t, 0.4H, J 7.8 Hz), 7.91 (d, 0.6H, J 8.2 Hz), 7.98 (d, 0.4H, J 8.2 Hz). Note: exchangeable protons (NH) were not apparent. The proton signals of two methylene groups (4 protons) of the fluorophore were not apparent due to an interference with the solvent residual peak. HRMS (ESI): m/z $[\text{M}]^+$ calcd. for $[\text{C}_{51}\text{H}_{64}\text{N}_7\text{O}_2]^+$: 806.5116, found 806.5121. RP-HPLC (220 nm): 97% (t_R = 9.6 min, k = 12.0). $\text{C}_{51}\text{H}_{64}\text{N}_7\text{O}_2\cdot\text{C}_2\text{F}_3\text{O}_2\cdot\text{C}_6\text{H}_3\text{F}_9\text{O}_6$ (807.12 + 455.09).

2-(6-(Dimethylamino)-3-(dimethyliminio)-3H-xanthen-9-yl)-5-((2-(4-(4-(1-(2-oxo-2-(11-oxo-10,11-dihydro-5H-dibenzo[*b,e*]-[1,4]diazepin-5-yl)ethyl)piperidin-4-yl)butyl)piperazin-1-yl)ethyl)carbamoyl)benzoate tris(hydrotrifluoroacetate) (20). Compound **20** was prepared from **10** (8.9 mg, 0.010 mmol) and **11** (4.1 mg, 0.0077 mmol) according to the procedure used for the synthesis of **15**. DIPEA: 11 mg, 14 μ L, 0.083 mmol. Purification of the product by preparative HPLC (gradient: 0–40 min: 0.1% aq TFA/acetonitrile 81:19–30:40, t_R = 13 min) yielded **20** as a red solid (6.5 mg, 66%). Ratio of configurational isomers evident in the $^1\text{H-NMR}$ spectrum: *ca.* 1.5:1. $^1\text{H-NMR}$ (600 MHz, $\text{MeOH-}d_4$): δ (ppm) 1.35–1.43 (m, 4H), 1.44–1.61 (m, 3H), 1.68–1.77 (m, 2H), 1.89–2.02 (m, 2H), 2.61 (brs, 2H), 2.83 (s, 2H), 2.86–3.00 (m, 1H), 3.00–3.12 (m, 4H), 3.45 (t, 2H, *J* 12 Hz, interfering with the ^{13}C satellite of the solvent residual peak), 3.66 (t, 2H, *J* 6.2 Hz), 3.70–3.83 (m, 2H), 4.40 (d, 0.6H, *J* 17 Hz), 4.44 (d, 0.4H, *J* 17 Hz), 7.00 (d, 2H, *J* 2.2 Hz), 7.05 (d, 0.8H, *J* 2.2 Hz), 7.07 (d, 1.2H, *J* 2.3 Hz), 7.13 (d, 2H, *J* 9.4 Hz), 7.25–7.36 (m, 2H), 7.39 (t, 0.4H, *J* 7.8 Hz), 7.47–7.56 (m, 3.2H), 7.60–7.67 (m, 1.4H), 7.70 (t, 0.6H, *J* 7.4 Hz), 7.76 (t, 0.4H, *J* 7.6 Hz), 7.91 (d, 0.6H, *J* 7.8 Hz), 7.98 (d, 0.4H, *J* 7.7 Hz), 8.23–8.28 (m, 1H), 8.77 (s, 1H). Note: exchangeable protons (NH, OH) were not apparent. The proton signals of the four methyl groups (12 protons) and four protons of the piperazine ring (CH_2 groups) were not apparent due to an interference with the solvent residual peak. HRMS (ESI): *m/z* $[\text{M} + \text{H}]^+$ calcd. for $[\text{C}_{55}\text{H}_{63}\text{N}_8\text{O}_6]^+$: 931.4865, found 931.4868. RP-HPLC (220 nm): 99% (t_R = 6.9 min, *k* = 8.1). $\text{C}_{55}\text{H}_{62}\text{N}_8\text{O}_6 \cdot \text{C}_6\text{H}_3\text{F}_3\text{O}_6$ (931.15 + 342.06).

Investigation of the chemical stability

The chemical stabilities of **15–20** were investigated in PBS pH 7.4 at 22 ± 1 °C using propylene vessels. The incubation was started by the addition of 10 μ L of 1 mM solution of the fluorescent ligand in DMSO to PBS (90 μ L) to yield a final concentration of 100 μM . After 0, 24 and 48 h, aliquots (20 μ L) were taken and added to 1% aq TFA/acetonitrile (8:2 v/v) (20 μ L). The resulting solutions were analyzed by RP-HPLC (analytical HPLC system and conditions see general experimental conditions; t_R : 7.8 min (**15**), 13.5 min (**16**), 9.95 min (**17**), 8.1 min (**18**), 10.0 min (**19**), 7.3 min (**20**)).

Cell culture

CHO-K9 cells, stably transfected with the DNA of human muscarinic receptors M_1 – M_5 (obtained from Missouri S&T cDNA Resource Center; Rolla, MO) were cultured in HAM's F12 medium supplemented with fetal calf serum (Biochrom, Berlin, Germany) (10%) and G418 (Biochrom) ($750 \mu\text{g mL}^{-1}$).

Determination of excitation and emission spectra

Excitation and emission spectra of compounds **15–20** were recorded in PBS, pH 7.4, containing 1% BSA (Serva, Heidelberg, Germany), at 22 °C with a Cary Eclipse spectrofluorimeter (Varian Inc., Mulgrave, Victoria, Australia) using acryl cuvettes (10 \times 10 mm, Ref. 67.755, Sarstedt,

Nümbrecht, Germany). The slit adjustments (excitation/emission) were 5/10 nm for excitation spectra and 10/5 nm in case of emission spectra. Net spectra were calculated by subtracting the respective vehicle reference spectrum, and corrected emission spectra were calculated by multiplying the net emission spectra with the respective lamp corrections spectrum (same slit adjustments, *etc.*).

Radioligand competition binding assay

Equilibrium competition binding studies with $[\text{}^3\text{H}]\text{NMS}$ were performed at intact CHO-h M_xR cells ($x = 1$ –5) at 23 ± 1 °C in white 96-wells plates with clear bottom (Corning Life Science, Tewksbury, MA; Corning cat. No. 3610) using Leibovitz's L-15 medium (Gibco, Life Technologies, Darmstadt, Germany) supplemented with 1% BSA (Serva) as binding buffer (in the following referred to as L15 medium). Experiments were performed using a previously described protocol for MR binding studies with $[\text{}^3\text{H}]\text{NMS}$,⁴³ but the total volume per well was 200 μL , *i.e.* wells were pre-filled with 180 μL of L15 medium followed by the addition of L15 medium (20 μL) containing $[\text{}^3\text{H}]\text{NMS}$ (10-fold concentrated), to determine total binding, or pre-filled with 160 μL of L15 medium followed by the addition of L15 medium (20 μL) containing atropine or the compound of interest (10-fold concentrated) and L15 medium (20 μL) containing $[\text{}^3\text{H}]\text{NMS}$ (10-fold concentrated), to determine unspecific binding and the displacing effect of a compound of interest, respectively. The concentrations of $[\text{}^3\text{H}]\text{NMS}$ were 0.2 nM ($\text{M}_{1\text{R}}$, $\text{M}_{2\text{R}}$, $\text{M}_{3\text{R}}$), 0.1 nM ($\text{M}_{4\text{R}}$) or 0.3 nM ($\text{M}_{5\text{R}}$). Samples were incubated in the dark under gentle shaking for 3 h. Prior to the competition binding experiments, the K_d values of $[\text{}^3\text{H}]\text{NMS}$ were determined by saturation binding applying the same conditions (buffer, temperature, incubation time, unspecific binding, *etc.*). The obtained K_d values amounted to 0.17 ± 0.01 nM ($\text{M}_{1\text{R}}$), 0.10 ± 0.01 nM ($\text{M}_{2\text{R}}$), 0.12 ± 0.01 nM ($\text{M}_{3\text{R}}$), 0.052 ± 0.01 nM ($\text{M}_{4\text{R}}$) and 0.20 ± 0.02 nM ($\text{M}_{5\text{R}}$) (mean value \pm SEM from at least four independent determinations performed in triplicate), being in excellent agreement with previously determined K_d values of $[\text{}^3\text{H}]\text{NMS}$.⁴³

Flow cytometric saturation binding experiments

Flow cytometric $\text{M}_{2\text{R}}$ binding studies were performed with a FACSCantoII flow cytometer (Becton Dickinson, Heidelberg, Germany) (compounds **7** and **15–19**) or with a FACSCalibur flow cytometer (Becton Dickinson) (**20**), both equipped with an argon laser (488 nm) and a red diode laser (640 and 635 nm, respectively). Fluorescence signals were recorded using the following instrument settings: compound **15**, excitation: 488 nm, emission: 585 ± 21 nm (PE channel), gain: 385–440 V; compound **16**, excitation: 633 nm, emission: 660 ± 10 nm (APC channel), gain: 480–510 V; compounds **7** and **17–19**, excitation: 488 nm, emission: 670 ± 65 nm (PerCP-Cy5.5 channel), gain: 430 V (**7**) or 465–485 V (**17–19**); compound **20**, excitation: 488 nm, emission: 585 ± 21 nm (FL-2), gain: 750 V.

Measurements were stopped after counting of 10 000 gated events at medium (7, 17–19) or high (20) flow rate.

All samples were prepared and incubated in 1.5 mL reaction vessels (Sarstedt). Cells were seeded in a 175 cm² culture flask 5–6 days prior to the experiment. On the day of the experiment, cells were treated with trypsin, detached and suspended in culture medium followed by centrifugation. The cell pellet was re-suspended in Leibovitz's L15 culture medium (Gibco, Life Technologies) supplemented with 1% BSA (Serva) (in the following referred to as L15 medium). The cell density was adjusted to 1×10^6 cells per mL. For the determination of total binding, 2 μ L of a solution of fluorescent ligand (100-fold concentrated compared to the final concentration) in DMSO/H₂O (1:1 v/v) and 2 μ L of DMSO/H₂O (1:4 v/v) were added to 200 μ L of the cell suspension. For the determination of unspecific binding (in the presence of atropine at 500-fold excess to the fluorescent ligand), 2 μ L of a solution of atropine (100-fold concentrated) in DMSO/H₂O (1:4 v/v) were added instead of neat DMSO/H₂O (1:4 v/v) (note: in case of 20, the sample volume was 500 μ L, *i.e.* 5 μ L instead of 2 μ L of ligand solution was added, and the excess of atropine was 1000-fold). Compound 15 was used at final concentrations of 0.23–50 nM, 20 was used at final concentrations of 0.04–20 nM, compounds 7 and 16–19 were used at final concentrations of 0.15–30 nM. Samples were incubated at 22 °C in the dark under gentle shaking for 2 h. All experiments were performed in duplicate.

Data processing

Retention (capacity) factors were calculated from retention times (t_R) according to $k = (t_R - t_0)/t_0$ (t_0 = dead time). Raw data from flow cytometric experiments were processed with FACSDiva Software (Becton Dickinson) (7, 15–19) or with FlowJo Software (FlowJo LLC, Ashland, OR) (20) to obtain arithmetic mean values of the areas of the signals detected in the respective channel (FACSCantoII) and geometric mean values of the height of the signals detected in channel FL-2 (FACSCalibur), respectively. Specific binding data from flow cytometric saturation binding experiments, obtained by subtracting unspecific binding data from total binding data, were plotted against the fluorescent ligand concentration and analyzed by a two-parameter equation describing hyperbolic binding (one site-specific binding; GraphPad Prism 5, GraphPad Software, San Diego, CA) in order to obtain K_d and B_{max} values. K_d values of individual experiments were transformed to pK_d values. Unspecific binding data were fitted by linear regression. Data from the radioligand ([³H]NMS) saturation⁴³ and competition⁴⁴ binding assays were processed as reported previously. pIC_{50} values were converted to pK_i values according to the Cheng-Prusoff equation⁵⁰ (logarithmic form). Propagated errors were calculated as described previously.⁴⁷

Author contributions

C. G. G., A. P. and X. S. synthesized the fluorescent ligands. C. G. G. performed radiochemical and flow cytometric

binding experiments and analysed the data. M.K. initiated the project and supervised the research. C. G. G. and M. K. wrote the manuscript. All authors have given approval to the final version of the manuscript.

Abbreviations used

CHO-cells	Chinese hamster ovary cells
DIPEA	Diisopropylethylamine
GPCR	G-Protein coupled receptor
k	Retention (or capacity) factor (HPLC)
K_d	Dissociation constant obtained from saturation binding experiment
MR	Muscarinic receptor
NMS	<i>N</i> -Methylscopolamine
PBS	Phosphate buffered saline
pK_d	Negative logarithm of the K_d in M
pK_i	Negative logarithm of the dissociation constant K_i (in M) obtained from a competition binding experiment
TFA	Trifluoroacetic acid
t_R	Retention time

Conflicts of interest

The authors declare no competing financial interest.

Acknowledgements

The authors thank Maria Beer-Krön, Brigitte Wenzl and Susanne Bollwein for excellent technical assistance. This work was funded by the Graduate Training Program GRK 1910 of the Deutsche Forschungsgemeinschaft (DFG).

Notes and references

- S. J. Briddon, B. Kellam and S. J. Hill, *Methods Mol. Cell. Biol.*, 2011, **746**, 211–236.
- L. A. Stoddart, L. E. Kilpatrick, S. J. Briddon and S. J. Hill, *Neuropharmacology*, 2015, **98**, 48–57.
- L. A. Stoddart, L. E. Kilpatrick and S. J. Hill, *Trends Pharmacol. Sci.*, 2018, **39**, 136–147.
- L. A. Stoddart, C. W. White, K. Nguyen, S. J. Hill and K. D. G. Pfleger, *Br. J. Pharmacol.*, 2016, **173**, 3028–3037.
- S. J. Briddon and S. J. Hill, *Trends Pharmacol. Sci.*, 2007, **28**, 637–645.
- J. G. Baker, R. Middleton, L. Adams, L. T. May, S. J. Briddon, B. Kellam and S. J. Hill, *Br. J. Pharmacol.*, 2010, **159**, 772–786.
- K. Kuder and K. Kiec-Kononowicz, *Curr. Med. Chem.*, 2008, **15**, 2132–2143.
- K. J. Kuder and K. Kiec-Kononowicz, *Curr. Med. Chem.*, 2014, **21**, 3962–3975.
- R. J. Middleton, S. J. Briddon, Y. Cordeaux, A. S. Yates, C. L. Dale, M. W. George, J. G. Baker, S. J. Hill and B. Kellam, *J. Med. Chem.*, 2007, **50**, 782–793.

- 10 R. J. Middleton and B. Kellam, *Curr. Opin. Chem. Biol.*, 2005, **9**, 517–525.
- 11 A. J. Vernall, S. J. Hill and B. Kellam, *Br. J. Pharmacol.*, 2014, **171**, 1073–1084.
- 12 M. Amon, X. Ligneau, J. C. Schwartz and H. Stark, *Bioorg. Med. Chem. Lett.*, 2006, **16**, 1938–1940.
- 13 L. Li, J. Kracht, S. Peng, G. Bernhardt and A. Buschauer, *Bioorg. Med. Chem. Lett.*, 2003, **13**, 1245–1248.
- 14 L. Li, J. Kracht, S. Peng, G. Bernhardt, S. Elz and A. Buschauer, *Bioorg. Med. Chem. Lett.*, 2003, **13**, 1717–1720.
- 15 S. F. Malan, A. van Marle, W. M. Menge, V. Zuliani, M. Hoffman, H. Timmerman and R. Leurs, *Bioorg. Med. Chem.*, 2004, **12**, 6495–6503.
- 16 S. X. Xie, G. Petrache, E. Schneider, Q. Z. Ye, G. Bernhardt, R. Seifert and A. Buschauer, *Bioorg. Med. Chem. Lett.*, 2006, **16**, 3886–3890.
- 17 M. Leopoldo, E. Lacivita, E. Passafiume, M. Contino, N. A. Colabufo, F. Berardi and R. Perrone, *J. Med. Chem.*, 2007, **50**, 5043–5047.
- 18 A. Tabor, S. Weisenburger, A. Banerjee, N. Purkayastha, J. M. Kaindl, H. Hubner, L. Wei, T. W. Gromer, J. Kornhuber, N. Tschammer, N. J. Birdsall, G. I. Mashanov, V. Sandoghdar and P. Gmeiner, *Sci. Rep.*, 2016, **6**, 33233.
- 19 S. Arttamangkul, V. Alvarez-Maubecin, G. Thomas, J. T. Williams and D. K. Grandy, *Mol. Pharmacol.*, 2000, **58**, 1570–1580.
- 20 G. Balboni, S. Salvadori, A. Dal Piaz, F. Bortolotti, R. Argazzi, L. Negri, R. Lattanzi, S. D. Bryant, Y. Jinsmaa and L. H. Lazarus, *J. Med. Chem.*, 2004, **47**, 6541–6546.
- 21 A. Drakopoulos, Z. Koszegi, Y. Lanoiselee, H. Hubner, P. Gmeiner, D. Calebiro and M. Decker, *J. Med. Chem.*, 2020, **63**, 3596–3609.
- 22 R. A. Houghten, C. T. Dooley and J. R. Appel, *Bioorg. Med. Chem. Lett.*, 2004, **14**, 1947–1951.
- 23 S. Dukorn, T. Littmann, M. Keller, K. Kuhn, C. Cabrele, P. Baumeister, G. Bernhardt and A. Buschauer, *Bioconjugate Chem.*, 2017, **28**, 1291–1304.
- 24 Y. Dumont, P. Gaudreau, M. Mazzuferi, D. Langlois, J. G. Chabot, A. Fournier, M. Simonato and R. Quirion, *Br. J. Pharmacol.*, 2005, **146**, 1069–1081.
- 25 M. Keller, D. Erdmann, N. Pop, N. Pluym, S. Teng, G. Bernhardt and A. Buschauer, *Bioorg. Med. Chem.*, 2011, **19**, 2859–2878.
- 26 M. Liu, R. R. Richardson, S. J. Mountford, L. Zhang, M. H. Tempone, H. Herzog, N. D. Holliday and P. E. Thompson, *Bioconjugate Chem.*, 2016, **27**, 2166–2175.
- 27 E. Schneider, M. Keller, A. Brennauer, B. K. Hoefelschweiger, D. Gross, O. S. Wolfbeis, G. Bernhardt and A. Buschauer, *ChemBioChem*, 2007, **8**, 1981–1988.
- 28 R. Ziemek, A. Brennauer, E. Schneider, C. Cabrele, A. G. Beck-Sickinger, G. Bernhardt and A. Buschauer, *Eur. J. Pharmacol.*, 2006, **551**, 10–18.
- 29 E. Kozma, P. S. Jayasekara, L. Squarzialupi, S. Paoletta, S. Moro, S. Federico, G. Spalluto and K. A. Jacobson, *Bioorg. Med. Chem. Lett.*, 2013, **23**, 26–36.
- 30 M. P. Faure, P. Gaudreau, I. Shaw, N. R. Cashman and A. Beaudet, *J. Histochem. Cytochem.*, 1994, **42**, 755–763.
- 31 M. Keller, K. K. Kuhn, J. Einsiedel, H. Hubner, S. Biselli, C. Mollereau, D. Wifling, J. Svobodova, G. Bernhardt, C. Cabrele, P. M. Vanderheyden, P. Gmeiner and A. Buschauer, *J. Med. Chem.*, 2016, **59**, 1925–1945.
- 32 C. Tahtaoui, I. Parrot, P. Klotz, F. Guillier, J. L. Galzi, M. Hibert and B. Ilien, *J. Med. Chem.*, 2004, **47**, 4300–4315.
- 33 L. H. Jones, A. Randall, C. Napier, M. Trevethick, S. Sreckovic and J. Watson, *Bioorg. Med. Chem. Lett.*, 2008, **18**, 825–827.
- 34 J. A. Hern, A. H. Baig, G. I. Mashanov, B. Birdsall, J. E. Corrie, S. Lazareno, J. E. Molloy and N. J. Birdsall, *Proc. Natl. Acad. Sci. U. S. A.*, 2010, **107**, 2693–2698.
- 35 T. A. Nenasheva, M. Neary, G. I. Mashanov, N. J. Birdsall, R. A. Breckenridge and J. E. Molloy, *J. Mol. Cell. Cardiol.*, 2013, **57**, 129–136.
- 36 A. Harris, S. Cox, D. Burns and C. Norey, *J. Biomol. Screening*, 2003, **8**, 410–420.
- 37 S. B. Daval, C. Valant, D. Bonnet, E. Kellenberger, M. Hibert, J. L. Galzi and B. Ilien, *J. Med. Chem.*, 2012, **55**, 2125–2143.
- 38 S. B. Daval, E. Kellenberger, D. Bonnet, V. Utard, J. L. Galzi and B. Ilien, *Mol. Pharmacol.*, 2013, **84**, 71–85.
- 39 K. A. Jacobson, B. Fischer and A. M. van Rhee, *Life Sci.*, 1995, **56**, 823–830.
- 40 Y. Karton, J. Baumgold, J. S. Handen and K. A. Jacobson, *Bioconjugate Chem.*, 1992, **3**, 234–240.
- 41 Y. Wang, Q. Gu, F. Mao, R. P. Haugland and M. S. Cynader, *J. Neurosci.*, 1994, **14**, 4147–4158.
- 42 M. S. Gitler, R. C. Reba, V. I. Cohen, W. J. Rzeszotarski and J. Baumgold, *Brain Res.*, 1992, **582**, 253–260.
- 43 M. Keller, C. Trankle, X. She, A. Pegoli, G. Bernhardt, A. Buschauer and R. W. Read, *Bioorg. Med. Chem.*, 2015, **23**, 3970–3990.
- 44 A. Pegoli, X. She, D. Wifling, H. Hubner, G. Bernhardt, P. Gmeiner and M. Keller, *J. Med. Chem.*, 2017, **60**, 3314–3334.
- 45 A. Pegoli, D. Wifling, C. G. Gruber, X. She, H. Hubner, G. Bernhardt, P. Gmeiner and M. Keller, *J. Med. Chem.*, 2019, **62**, 5358–5369.
- 46 X. She, A. Pegoli, J. Mayr, H. Hubner, G. Bernhardt, P. Gmeiner and M. Keller, *ACS Omega*, 2017, **2**, 6741–6754.
- 47 X. She, A. Pegoli, C. G. Gruber, D. Wifling, J. Carpenter, H. Hübner, J. Wan, G. Bernhardt, P. Gmeiner, N. D. Holliday and M. Keller, *J. Med. Chem.*, 2020, **63**, 4133–4154.
- 48 B. K. Hoefelschweiger, *PhD thesis*, University of Regensburg, 2005, <http://d-nb.info/975903071/34>.
- 49 A. Rinken, D. Lavogina and S. Kopanchuk, *Trends Pharmacol. Sci.*, 2018, **39**, 187–199.
- 50 Y.-C. Cheng and W. H. Prusoff, *Biochem. Pharmacol.*, 1973, **22**, 3099–3108.